

The Bound Band Structure in a Strong Attractive Dirac Comb

Sid A. Sfiat

Faculté de physique, BP 1505 El Mnaouar, USTO-MB, 31000 Oran, Algeria.

Doi: <https://doi.org/10.47011/17.3.3>

Received on: 09/04/2022;

Accepted on: 12/01/2023

Abstract: The Dirac comb problem in quantum mechanics is revisited by estimating its energy band structure, including the band gap, bandwidth, and the effective mass at band edges. The case of an attractive strong Dirac comb potential is considered. Our findings show the existence of a single bound energy band state, which is flat with a small width and a large effective mass at both of its edges; positive at its lower edge and negative at its upper edge.

Keywords: Dirac comb, Bound energy, Band structure, Dispersion relation, Band gap, Bandwidth, Effective mass.

1. Introduction

In quantum mechanics, only a handful of problems can be solved analytically. One of these problems is the Kronig-Penney potential, introduced in the early 1930s to model the short-range nature of the atomic potentials and the periodic lattice structure [1]. A year later, Kronig and Penney simplified the original model and introduced the Dirac comb potential, which consists of one-dimensional evenly spaced delta-function peaks. This model is suitable for obtaining many general properties of realistic quantum systems. It is a solvable model frequently used to describe systems with very short-range interactions which are located around evenly spaced given points [2, 3].

The impressive progress in experimental physics in the early 1980s, coupled with the advances in semiconductor technology and nanophysical systems twenty years later, made possible the fabrication of heterostructures, quantum wells, and new synthetic materials. This renewed the interest of scientists and engineers in this elementary type of simple model [4, 5]. It has contributed immensely to explaining the electronic band structure in a crystalline solid such as band gap formation [4,

5]. This has led to a huge advancement in solid-state and condensed-matter physics. Many macroscopic properties of materials are closely related to their microscopic band structures. They are of extreme practical importance because they play a major role in understanding the transport phenomena theory of insulation and conduction in solids [6-11].

Because material properties are strongly influenced by energy band patterns, many physical properties of solids are determined from the location of band edges, band gaps, and their widths [6-11]. The goal of this work is to estimate the energy band structure (band gap, bandwidth, and effective mass) of an electron under the influence of a strong attractive Dirac comb potential. Similar attempts have been made for bound and unbound band structures under the influence of a weak attractive Dirac comb potential [12, 13].

2. Band Gap and Band Width Calculation

One of the few problems in quantum mechanics that can be solved analytically is the Dirac comb [14-17]. This work considers only

the attractive case of this model, where the associated potential is expressed as:

$$V(x) = -\lambda \sum_n^\infty \delta(x - na) \quad (1)$$

with strength λ and lattice spacing a .

Only the bound states are considered and therefore the electron energy is negative and expressed as:

$$E = -\frac{\hbar^2 K^2}{2m} \quad (2)$$

K is related to the Bloch wave number k through the following transcendental equation [14-17]:

$$-P \frac{\sinh(Ka)}{Ka} + \cosh(Ka) = \cos(ka) \quad (3)$$

where $P = \frac{ma\lambda}{\hbar^2}$ is a dimensionless parameter representing the scattering power of the Dirac comb potential.

Equation (3) determines the permitted energies E through the values of the parameter K . This transcendental equation cannot be solved analytically; it can only be solved numerically or graphically.

These permitted energies are determined because the right-hand side of Eq. (3) is bounded:

$$-1 \leq \cos(ka) \leq 1 \quad (4)$$

Analyzing Eq. (3) numerically (see Table 1) and graphically (Figs. 1-5), we note the following facts:

- A single bound energy band is formed, regardless of the value of the scattering power P .
- The band is partial and not complete when $0 < P < 2$. It does not span the entire half-interval of the first Brillouin zone from 0 to π , but rather the interval from 0 to $\arccos(1-P)$.
- The band is complete and spans the whole half-interval of the first Brillouin zone from 0 to π when $P \geq 2$.
- The band width increases very fast when $0 < P < 2$.
- The band width reaches its maximum value when $P = 2$.
- The band width decreases at a slower rate than the initial increase when $P > 2$.
- The band width almost vanishes and cannot be detected when $P \geq 15$.

TABLE 1. The energies at both ends of the band and its width

P	$(Ka)_0$	$(Ka)_\pi$	$E_0(\frac{\hbar^2}{2ma^2})$	$E_\pi(\frac{\hbar^2}{2ma^2})$	$W(\frac{\hbar^2}{2ma^2})$
0	0	x	0		0
0.5	1.04363	x	-1.08916	0	1.08916
1.0	1.54340	x	-2.38208	0	2.38208
1.5	1.98036	x	-3.92183	0	3.92183
2.0	2.39936	0	-5.75693	0	5.75693
2.5	2.81770	1.77603	-7.93943	-3.15428	4.78515
3.0	3.24364	2.57568	-10.52100	-6.63413	3.88687
3.5	3.68095	3.23488	-13.54939	-10.46445	3.08494
4.0	4.13068	3.83007	-17.06252	-14.66944	2.39308
4.5	4.59212	4.38973	-21.08757	-19.26973	1.81784
5.0	5.06363	4.92812	-25.64035	-24.28637	1.35398
10.0	10.0090	9.99909	-100.18008	-99.98009	0.19999
15.0	15.0000	15.0000	-225.0000	-225.0000	0

* Numerical values in Table 1 are provided by dCode equation solver tool.

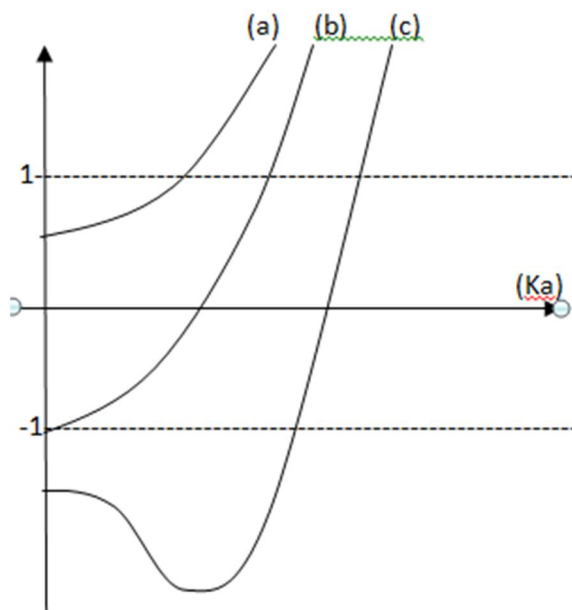


FIG. 1. The function " $-P \frac{\sinh(Ka)}{Ka} + \cosh(Ka)$ " versus Ka for (a) $0 < P < 2$, (b) $P = 2$, (c) $P > 2$.

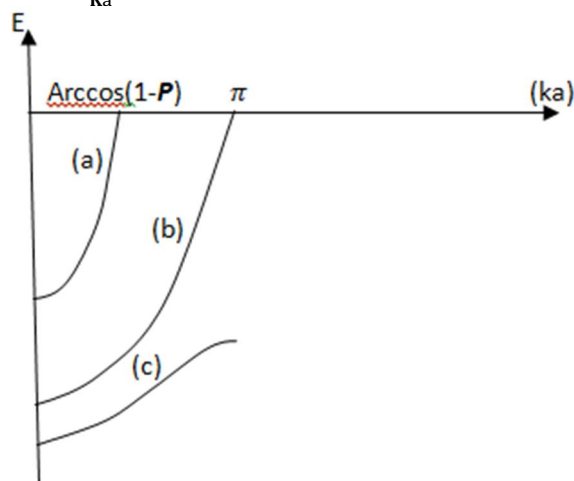


FIG. 2. Dispersion relation versus ka for (a) $0 < P < 2$, (b) $P = 2$, (c) $P > 2$.

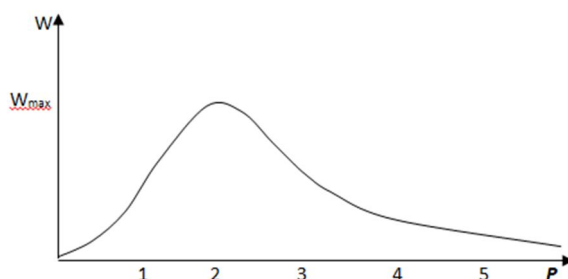


FIG. 3. The band width as a function of the scattering power P .

The case of the strong Dirac comb potential is considered in this work and therefore the scattering power $P \gg 1$.

Analyzing Fig. 4 below, we notice that the left-hand side of Eq. (3) intersects the axis Ka at a value very close to P . It also intersects the horizontal lines representing the points $ka = 0$ and $ka = \pi$ at:

$$K_0 a = P + \delta_0 \tag{5}$$

and

$$K_\pi a = P - \delta_\pi \tag{6}$$

respectively, where $0 \leq \delta_0 \ll 1$ and $0 \leq \delta_\pi \ll 1$.

Inserting Eq. (5) into Eq. (3) when $ka = 0$, we get:

$$-P \frac{\sinh(P+\delta_0)}{(P+\delta_0)} + \cosh(P + \delta_0) = 1 \quad (7)$$

Solving for δ_0 to the first-order approximation, yields [18, 19]:

$$\delta_0 \approx 2Pe^{-P} \quad (8)$$

Therefore,

$$K_0 a \approx P(1 + 2e^{-P}) \quad (9)$$

The lowest energy of the band is at:

$$E_0 = -\frac{\hbar^2 K_0^2}{2m} \approx -\frac{\hbar^2 P^2(1+4e^{-P})}{2ma^2} \quad (10)$$

Similarly, for $ka = \pi$, the same approach yields:

$$\delta_\pi \approx 2Pe^{-P} \quad (11)$$

and

$$K_\pi a \approx P(1 - 2e^{-P}) \quad (12)$$

The highest energy of the band is at:

$$E_\pi = -\frac{\hbar^2 K_\pi^2}{2m} \approx -\frac{\hbar^2 P^2(1-4e^{-P})}{2ma^2} \quad (13)$$

Therefore, the width of the band is:

$$W = E_\pi - E_0 = \frac{4\hbar^2 P^2 e^{-P}}{ma^2} \quad (14)$$

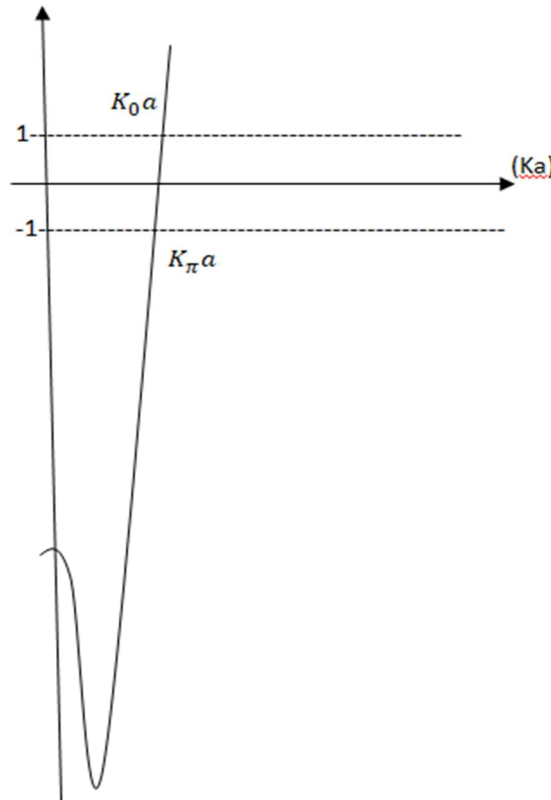


FIG. 4. The function " $-P \frac{\sinh(Ka)}{Ka} + \cosh(Ka)$ " versus Ka for large values of P .

Fig. 5 below shows the dispersion relation. It consists of a single bound energy band lying very far below the zero line. It is almost flat,

with its width decreasing with increasing values of the scattering power P .

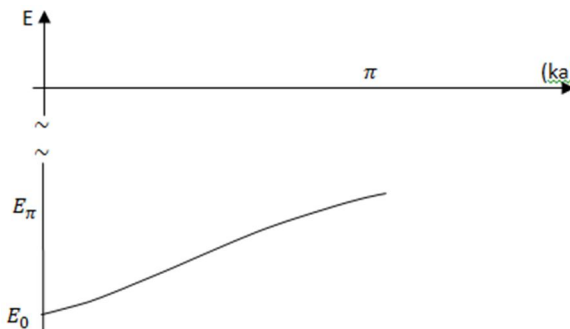


FIG. 5. The dispersion relation versus ka for large values of P .

Let us now find an analytical approximation for the dispersion relation $E(\mathbf{k})$. For that, we make use of the observation made from the graph in Fig. 4. The left-hand side of Eq. (3), between the two horizontal lines representing the points $\mathbf{ka} = 0$ and $\mathbf{ka} = \pi$, can be approximated by a straight line passing through points $(\mathbf{K}_\pi a, -1)$, $(\mathbf{P}, 0)$, and $(\mathbf{K}_0 a, 1)$. Hence, this side of Eq. (3) can be expressed as:

$$\text{L. H. S} = \frac{1}{\delta_0} (\mathbf{K}a - \mathbf{P}) \quad (15)$$

and this leads to:

$$\mathbf{K}a = \delta_0 \cos(\mathbf{ka}) + \mathbf{P} \quad (16)$$

Therefore, the energy $E(\mathbf{k})$ can be expressed as a function of the Bloch wave number \mathbf{k} as:

$$E(\mathbf{ka}) = -\frac{\hbar^2 p^2}{2ma^2} [2e^{-P} \cos(\mathbf{ka}) + 1]^2 \quad (17)$$

The width of the band can also be expressed as:

$$W = E(\pi) - E(0) = \frac{4\hbar^2 p^2 e^{-P}}{ma^2} \quad (18)$$

The above dispersion relation $E(\mathbf{ka})$ will be used in the next section to confirm and verify the final findings regarding the effective mass estimations. It is worth noting that Eqs. (17) and (18) are compatible with the results obtained in Eqs. (10) and (13) when the scattering power $P \gg 1$.

With increasing scattering power P , the dependence of the above dispersion relation $E(\mathbf{ka})$ on the Bloch wave number \mathbf{k} weakens and becomes practically undetectable beyond $P = 15$, where the energy band collapses to a single energy level $E = -\frac{\hbar^2 p^2}{2ma^2}$. This energy is similar to that of a particle under the influence of a single delta function potential. Consequently, this form of energy confinement leads to a spatial localization phenomenon near the delta spike.

3. Effective Mass Calculation

The effective mass is an important tool in the theory of solids. It is used to describe the features of band structure in semiconductors and insulators, where most experimental features arise from electron and hole occupation near the endpoints of valence and conduction bands [20-23]. In this section, we evaluate the effective mass at both edges of the single bound energy band found in the previous section.

- The lowest edge of the band: $\mathbf{ka} = 0$.

This edge corresponds to:

$$\mathbf{K}a = \mathbf{K}_0 a - \epsilon(\mathbf{ka}) \quad (19)$$

with $\epsilon(\mathbf{ka}) \ll 1$ and $\epsilon(0) = 0$

The corresponding energy is expressed as:

$$E_0 = -\frac{\hbar^2 \mathbf{K}^2}{2m} = -\frac{\hbar^2}{2ma^2} [\mathbf{K}_0 a - \epsilon]^2 \quad (20)$$

Combining Eqs. (19) and (3) yields:

$$-P \frac{\sinh(\mathbf{K}_0 a - \epsilon)}{(\mathbf{K}_0 a - \epsilon)} + \cosh(\mathbf{K}_0 a - \epsilon) - 1 = \delta(\mathbf{ka}) \quad (21)$$

where

$$\delta(\mathbf{ka}) = -1 + \cos(\mathbf{ka}) \quad (22)$$

Expanding the above expression for $\delta(\mathbf{ka})$ in Eq. (21) as a Taylor power series in $\epsilon \ll 1$ yields:

$$\delta(\mathbf{ka}) = \frac{[(\mathbf{K}_0 a) \cosh(\mathbf{K}_0 a) - \sinh(\mathbf{K}_0 a)] P - (\mathbf{K}_0 a)^2 \sinh(\mathbf{K}_0 a)}{(\mathbf{K}_0 a)^2} \epsilon + O(\epsilon^2) \quad (23)$$

Using the Taylor reversion process for Eq. (23) yields [18, 19]:

$$\epsilon = \frac{(\mathbf{K}_0 a)^2}{[(\mathbf{K}_0 a) \cosh(\mathbf{K}_0 a) - \sinh(\mathbf{K}_0 a)] P - (\mathbf{K}_0 a)^2 \sinh(\mathbf{K}_0 a)} \delta + O(\delta^2) \quad (24)$$

By using Eqs. (20), (22), and (24), the effective mass expression at the lowest edge of the band becomes:

$$\left[\frac{d^2 E}{dk^2} \right]_0 = \frac{\hbar^2}{m^*} = -\frac{\hbar^2}{m} \frac{(\mathbf{K}_0 a)^3}{[(\mathbf{K}_0 a) \cosh(\mathbf{K}_0 a) - \sinh(\mathbf{K}_0 a)] P - (\mathbf{K}_0 a)^2 \sinh(\mathbf{K}_0 a)} \quad (25)$$

Hence, at the bottom of the band, the ratio (m^*/m) of the effective mass to the mass of the electron is expressed as:

$$\left[\frac{m^*}{m} \right]_0 = -\frac{[(\mathbf{K}_0 a) \cosh(\mathbf{K}_0 a) - \sinh(\mathbf{K}_0 a)] P - (\mathbf{K}_0 a)^2 \sinh(\mathbf{K}_0 a)}{(\mathbf{K}_0 a)^3} \quad (26)$$

Using Eq. (9) and the fact that $P \gg 1$, the effective mass ratio can be simplified to:

$$\left[\frac{m^*}{m} \right]_0 \approx \frac{e^P}{2P^2} \quad (27)$$

The dispersion relation (17) is now used to verify and confirm the result of Eq. (27):

$$\left[\frac{d^2E}{dk^2}\right]_0 = \frac{\hbar^2}{m^*} = 2 \frac{\hbar^2}{m} P^2 e^{-P} (1 + e^{-P}) \quad (28)$$

Therefore, the effective mass ratio (m^*/m) is estimated as:

$$\left[\frac{m^*}{m}\right]_0 \approx \frac{e^P}{2P^2} (1 - e^{-P}) \approx \frac{e^P}{2P^2} \quad (29)$$

which is exactly what was found in Eq. (27).

In conclusion, the effective mass at the lowest edge of the band is positive and large in value.

- The highest edge of the band: $\mathbf{k}a = \pi$.

This edge corresponds to:

$$\mathbf{K}a = \mathbf{K}_\pi a + \epsilon(\mathbf{k}a) \quad (30)$$

with $\epsilon(\mathbf{k}a) \ll 1$ and $\epsilon(\pi) = 0$

The corresponding energy is expressed as:

$$E_\pi = -\frac{\hbar^2 K^2}{2m} = -\frac{\hbar^2}{2ma^2} [\mathbf{K}_\pi a + \epsilon]^2 \quad (31)$$

Combining Eqs. (28) and (3) yields:

$$-P \frac{\sinh(\mathbf{K}_\pi a + \epsilon)}{(\mathbf{K}_\pi a + \epsilon)} + \cosh(\mathbf{K}_\pi a + \epsilon) + 1 = \Delta(\mathbf{k}a) \quad (32)$$

where:

$$\Delta(\mathbf{k}a) = 1 + \cos(\mathbf{k}a) \quad (33)$$

Expanding the above expression $\Delta(\mathbf{k}a)$ in Eq. (32) as a Taylor power series in $\epsilon \ll 1$ yields:

$$\Delta(\mathbf{k}a) = -\frac{[(\mathbf{K}_\pi a) \cosh(\mathbf{K}_\pi a) - \sinh(\mathbf{K}_\pi a)] P - (\mathbf{K}_\pi a)^2 \sinh(\mathbf{K}_\pi a)}{(\mathbf{K}_\pi a)^2} \epsilon + O(\epsilon^2) \quad (34)$$

Using the Taylor reversion process for Eq. (34) yields [18, 19]:

$$\epsilon = -\frac{(\mathbf{K}_\pi a)^2}{[(\mathbf{K}_\pi a) \cosh(\mathbf{K}_\pi a) - \sinh(\mathbf{K}_\pi a)] P - (\mathbf{K}_\pi a)^2 \sinh(\mathbf{K}_\pi a)} \Delta + O(\Delta^2) \quad (35)$$

By using Eqs. (31), (33), and (35), the effective mass expression at the highest edge of the band becomes:

$$\left[\frac{d^2E}{dk^2}\right]_\pi = \frac{\hbar^2}{m^*} = \frac{\hbar^2}{m} \frac{(\mathbf{K}_\pi a)^3}{[(\mathbf{K}_\pi a) \cosh(\mathbf{K}_\pi a) - \sinh(\mathbf{K}_\pi a)] P - (\mathbf{K}_\pi a)^2 \sinh(\mathbf{K}_\pi a)} \quad (36)$$

Hence, at the top of the band, the ratio (m^*/m) of the effective mass to the mass of the electron is expressed as:

$$\left[\frac{m^*}{m}\right]_\pi = \frac{[(\mathbf{K}_\pi a) \cosh(\mathbf{K}_\pi a) - \sinh(\mathbf{K}_\pi a)] P - (\mathbf{K}_\pi a)^2 \sinh(\mathbf{K}_\pi a)}{(\mathbf{K}_\pi a)^3} \quad (37)$$

Using Eq. (12) and the fact that $P \gg 1$, the effective mass ratio simplifies to:

$$\left[\frac{m^*}{m}\right]_\pi \approx -\frac{e^P}{2P^2} \quad (38)$$

Let us now use the dispersion relation (17) to verify and confirm the result of Eq. (38):

$$\left[\frac{d^2E}{dk^2}\right]_\pi = \frac{\hbar^2}{m^*} = -2 \frac{\hbar^2}{m} P^2 e^{-P} (1 - e^{-P}) \quad (39)$$

Therefore, the effective mass ratio (m^*/m) is estimated as:

$$\left[\frac{m^*}{m}\right]_\pi \approx -\frac{e^P}{2P^2} (1 + e^{-P}) \approx -\frac{e^P}{2P^2} \quad (40)$$

which is exactly what we have found in Eq. (38)

In conclusion, the effective mass at the highest edge of the band is negative and large in value.

4. Discussion and Conclusion

Under the influence of an attractive Dirac comb potential, an electron exhibits a single-bound band structure.

With increasing values of the scattering power P , the bandwidth initially increases rapidly for $0 < P < 2$ and then decreases at a slower rate when $P > 2$. The band is at its maximum width at $P = 2$.

When the scattering power P is very large, the band is found to be lying below the zero line of the reference energy. The band becomes nearly flat, with a weak dependence on the Bloch wave number. As a result, it collapses into an energy level of a particle under the influence of a single delta function potential, with its energy confinement and spatial localization phenomenon.

The dispersion relation is estimated and used to verify and confirm the findings regarding the effective mass at both ends of this single band. The effective mass is found to be very large, positive at the band's lowest edge, and negative at its highest edge.

Future investigations will aim to answer the following important questions: Can we expect similar results in the original case of the Kronig-Penney potential? If so, what conditions on the

size and depth of the well must be met for the single band to exhibit a similar pattern as in the Dirac comb potential?

References

- [1] Kronig, R.de L. and Penney, W.G., Proc. Roy. Soc. London, A130 (1930), 499.
- [2] Flugge, S., "Practical Quantum Mechanics", (Berlin: Springer-Verlag, 1971).
- [3] Ashcroft, N.W. and Mermin, N.D., "Solid State Physics", (Brooks/Cole, 1976).
- [4] Kolbas, R.M. and Holonyak, N., Amer. J. Phys., 52 (1984) 431.
- [5] Mitin, V.V., Sementsov, D.I., and Vagidov, N.Z., "Quantum Mechanics for Nanostructures", (Cambridge University Press, 2010).
- [6] Harrison, W.A., "Electronic Structure and the Properties of Solids", (ISBN 0-486-66021-4), (Dover, 1980).
- [7] Pastori Parravicini, G., "Electronic States and Optical Transitions in Solids". (Pergamon Press, 1975).
- [8] Dharani, M. and Shastry, C.S., Physica B, 500 (2016) 66.
- [9] Dharani, M. and Shastry, C.S., Mater. Today: Proc., Part 3, 5 (8) (2018) 16214.
- [10] Erman, F., Gadella, M. and Uncu, H., Eur. J. Phys., 39 (2018) 01.
- [11] Nussbaum, A., IEEE Trans. Educ., 33 (4) (1990) 359.
- [12] Sfiat, S., Adv. Stud. Theor. Phys., 7 (13) (2013) 605.
- [13] Sfiat, S., Adv. Studies Theory. Phys., 7 (13) (2013) 611.
- [14] Dekker, A.J., "Solid State Physics", (Prentice-Hall, Englewood Cliffs, NJ, 1962).
- [15] Kittel, C., "Quantum Theory of Solids", (John Wiley and Sons, New York, 1976).
- [16] Kittel, C. "Introduction to Solid State Physics", 7th Ed., (New York, Wiley, 1996).
- [17] Griffiths, D., "Introduction to Quantum Mechanics", (Cambridge University Press, UK, 2016).
- [18] Dwight, H.B., "Table of Integrals and Other Mathematical Data", 4th Ed., (New York: Macmillan, 1961).
- [19] Bronstein, I.N., Semendyayev, K.A., Musiol, G., and Muehlig, H., "Handbook of Mathematics". (Berlin, Heidelberg, New York, Springer, 2004).
- [20] Pekar, S., Zh. Eksp. Teor. Fiz., 16 (1946) 933.
- [21] Burt, M.G., J. Phys.: Condens. Matter, 4 (32) (1992) 6651.
- [22] Wasserman et al., Adv. Phys., 45 (1996) 471.
- [23] Sputai, S.V., XIV International Scientific-Technical Conference on Actual Problems of Electronics Instrument Engineering (APEIE), (2018), p. 178.